

GROWING AND CHARACTERIZATION OF Cs₂Te PHOTOCATHODES WITH DIFFERENT THICKNESSES AT INFN LASA

L. Monaco*, P. Michelato, D. Sertore, INFN LASA, Segrate, Italy
 C. Pagani, G. Guerini Rocco, Università degli Studi di Milano e INFN LASA, Segrate, Italy

Abstract

The INFN LASA group has a long standing experience in the production of cesium telluride photocathodes for high brightness photoinjectors. The well-established recipe relies on the deposition of a typical amount of 10 nm of Te, followed by the Cs deposition until reaching the maximum QE. Nevertheless, for improving the understanding of photocathode properties, we are investigating the effect of Te thickness on the growing process, evaluating photocathode optical properties and quantum efficiency during the growing process and on the final film. These photocathodes will be then operated and analyzed in the real environment of the RF Gun at the PITZ facility in DESY Zeuthen, to estimate their impact on the electron beam properties.

INTRODUCTION

The INFN LASA activities on photocathodes to be used in high brightness photoinjectors started in the '90s in the framework of the TESLA collaboration. After a first phase mainly dedicated to R&D studies, we started the production of Cs₂Te photocathodes and we delivered the first photocathodes in 1998 to the TTF RF Gun at DESY-Hamburg. Since then, we continuously produced photocathodes, reaching now a total delivery of about 150 Cs₂Te films, distributed to several laboratories such DESY-Hamburg for FLASH, DESY-Zeuthen for PITZ, LBNL for APEX and, SLAC for the commissioning of LCLS-II photoinjector.

The need to satisfy requests for usage of our photocathodes in RF guns of accelerators and user facilities guided our activity to develop reproducible and robust recipe, able to furnish the needed Quantum Efficiency (QE) for the operation, a good QE spatial uniformity, a long operative lifetime and a low dark current (DC). All these issues were reached [1] and, as an example, the operative lifetime was increased from few months to few years (24/7) [2]. The development of a multi-wavelength technique for monitoring QE and reflectivity during cathode formation improved further the reproducibility of the final photocathodes [3].

In this paper, we present the results obtained on photocathodes produced with different Te layer thicknesses and we compared them with the properties of our well known standard cathodes. Moreover, these photocathodes have then been used at PITZ for their characterization in the RF Gun, in the framework of the INFN LASA and DESY PITZ collaboration and the results are presented at this conference [4].

* laura.monaco@mi.infn.it

CATHODE DEPOSITION AND DIAGNOSTIC

Photoemissive films are evaporated sequentially on high purity Mo plugs (99.95 %), optically polished (typical roughness R_a = 10 nm). The deposition is done in the preparation chamber (base pressure 1 × 10⁻¹⁰ mbar) with a diameter of 5 mm realized with a Mo masking system. After an heating cycle up to 450 °C, the plug is cooled to 120 °C and the Te deposition starts (1 nm/min). When 10 nm of Te are deposited, the Cs deposition starts at 1 nm/min and ends when the QE reaches the typical maximum [5]. For the purpose of this work, we have grown photocathodes with 5 nm and 15 nm of Te besides a standard "10 nm". In all cases, the Cs deposition stopped when the QE reached its maximum.

Reflectivity

During the film growth, the plug is illuminated at different wavelengths, with a spot of approximately 5 mm (corresponding to the active area) to ensure a uniform reaction of the entire film area. The reflected power is extremely useful especially for the control of the real amount of Te deposited on the plug surface. Figure 1 reports the reflectivity variation for three different Te thicknesses and the theoretical predictions based on tabulated values for Mo and Te [6], in the assumption of a formation of a uniform Te layer on top of Mo substrate. The deviation from theory at thicker layers is possibly due to formation of islands of Te on Mo that our model does not take into account.

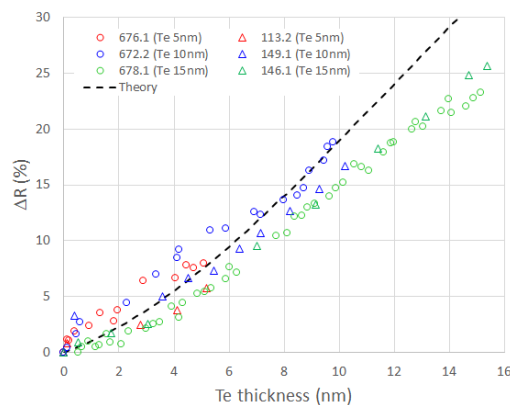


Figure 1: Te reflectivity decrease (ΔR) for three different film thickness and the expectation from tabulated values.

Table 1 reports the average reflectivity variation for the three different types of photocathodes based on all measurements so far available (26 films for "10 nm", 3 films for "5 nm" and "15 nm").

Content from this work may be used under the terms of the CC BY 3.0 licence (© 2019). Any distribution of this work must maintain attribution to the author(s), title of the work, publisher, and DOI

Table 1: Average Reflectivity Variation During Te Deposition

	5 nm	10 nm	15 nm
ΔR	$7.0 \pm 0.8 \%$	$16.8 \pm 2.2 \%$	$27.5 \pm 3.0 \%$
ΔR_{theory}	7.4 %	19.1 %	31.7 %

During the Cs deposition, the Te film reacts with Cs and different stoichiometric compounds grow until Cs_2Te is formed [7]. The evolution of the reflectivity at 254 nm for "5 nm", "10 nm" and "15 nm" photocathode is shown in Fig. 2 where the typical oscillation due to interference patterns of the thin film formation are clearly visible. Moreover, the "5 nm" photocathode shows a decrease of the reflectivity near to photocathode completion while the other two go asymptotically to a final reflectivity value for Cs_2Te of about 18%. These measurements confirm the results obtained on a similar set of photocathodes with different thickness we produced some years ago [8].

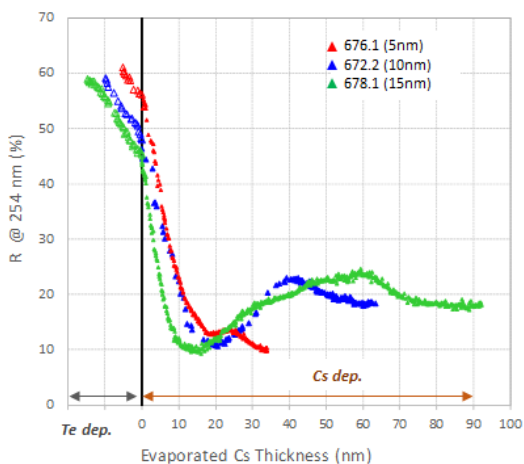


Figure 2: Reflectivity at 254 nm during Cs evaporation.

Finally Fig. 3 shows the reflectivity measured during Cs deposition at all the wavelengths available in our set-up. The minimum in reflectivity is reached firstly by shorter wavelengths as well as the following maxima. This behaviour is common to the three films and it depends on Te thickness. However, even the "15 nm" film is not thick enough to avoid the presence of the interference pattern.

Quantum Efficiency

As for the reflectivity, the photocurrent at different wavelengths is also a powerful tool to detect the complete formation of the Cs_2Te films since its last peak is more pronounced at longer wavelengths [3, 8]. This technique improves also the reproducibility of the recipe and the final QE of the photocathodes. Indeed, Table 2 reports the thickness of Te and Cs evaporated for the three typologies of photocathodes (26 films for 10 nm, 3 films for 5 nm and 15 nm) showing a nearly constant ratio between the two materials. As in previous measurements, the appearance of the typical plateaus

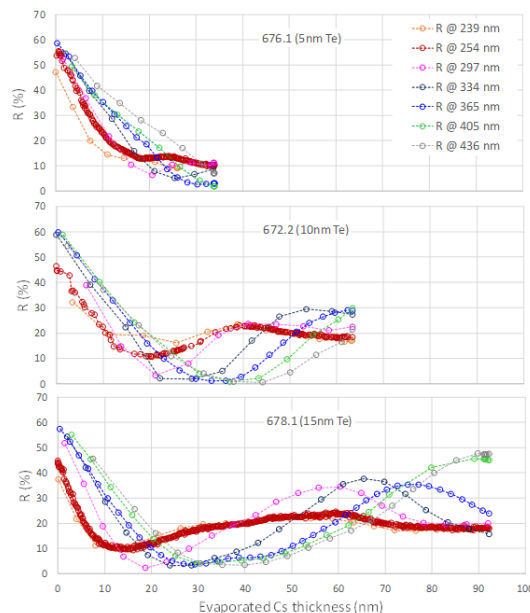


Figure 3: Reflectivity during Cs evaporation at all available wavelengths.

happens at the same Te/Cs ratio for the three photocathodes, independently from the Te thickness.

Table 2: Evaporated Te and Cs Thickness

	5 nm	10 nm	15 nm
Te	$5.1 \pm 0.1 \text{ nm}$	$9.7 \pm 0.3 \text{ nm}$	$15.1 \pm 0.2 \text{ nm}$
Cs	$33.8 \pm 0.5 \text{ nm}$	$60.4 \pm 2.8 \text{ nm}$	$89.9 \pm 3.0 \text{ nm}$

FILM CHARACTERIZATION, DIAGNOSTIC AND RESULTS

After production, no further analysis is done in the preparation chamber, and the coated plugs are moved back into the transport box. This box is a modified six-way cross used for delivering the photocathodes from the production system to the RF guns and it is equipped with a Sapphire viewport, transparent to UV, and with an anode for the collection of the photoelectrons. This configuration is used both for QE and reflectivity measurements (see Table 3 for final values) in a more suited environment than the preparation chamber. Two motorized mirrors mounted outside the box allow mapping QE of the coated area for all the available wavelengths ($\phi = 1 \text{ mm}$ and step 0.5 mm).

QE and Spectral Response

Spectral response (QE at different wavelengths) is a valid tool to monitor the reproducibility of the photocathodes produced. Moreover, it gives an indication on the photoemission threshold (minimum photon energy for emitting an electron) of the produced materials [9].

Figure 4 shows the spectral responses for the three different photocathodes. While all show comparable QE values,

the thinner one shows a slight "shoulder" at low energy probably due to Cs excess during deposition. Indeed, the determination of the "peak" to stop the Cs evaporation is more difficult in this case due to the thin Te layer.

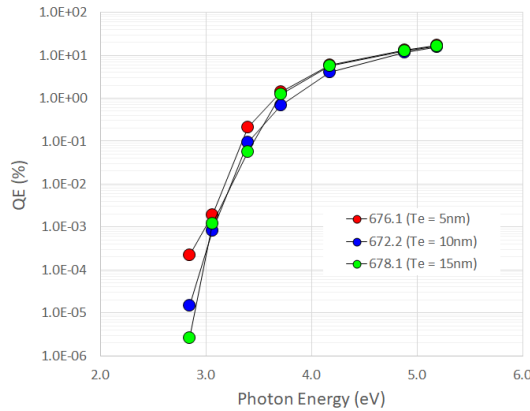


Figure 4: Spectral responses just after the deposition for the three films.

QE maps and Energy Threshold ($E_g + E_a$)

As introduced before, the analysis of the spectral response allows estimating the $E_g + E_a$ (Energy Gap + Electron Affinity) of the Cs_2Te . We have applied this technique to the whole photocathode area. We acquired photocathode maps at different wavelengths and from them we fit the QEs for every single spot and estimate the photocathode $E_g + E_a$ applying the following formula as reported in Kane [10] and adapted for a possible lower energy threshold:

$$QE = A[h\nu - (E_g + E_a)]^m + B[h\nu - (E_{g1} + E_{a1})]^{m1} \quad (1)$$

where A and B are adapting constant, $h\nu$ the photon energy, $E_g + E_a$ and $E_{g1} + E_{a1}$ are the corresponding energy gap and electron affinity and, m and m1 the power coefficients that, in Kane theory, are linked to the transition type in the semiconducting film.

Figure 5 reports the maps for the three photocathodes. The upper row is the $E_g + E_a$ over the photocathode area (the Mo substrate is set top 4.5 eV by default) only for the first term in Eq. 1, middle row is the QE map at 254 nm and the lower row QE map at 365 nm. Besides the QE map uniformity, the maps at 254 nm are not sensitive enough to the $E_g + E_a$ variation. On the contrary, maps at 365 nm show a quite good correlation with the $E_g + E_a$ maps. As expected regions of lower QE correspond to higher $E_g + E_a$ area as clearly shown for the "10 nm" photocathode (middle columns in Fig. 5) where the lower left area shows lower QE in the 365 nm map as well as high $E_g + E_a$ values.

Reflectivity

The final reflectivities of the three cathodes are reported in Fig. 6. These values agree with the one obtained on a similar set of photocathodes produced in the past [8].

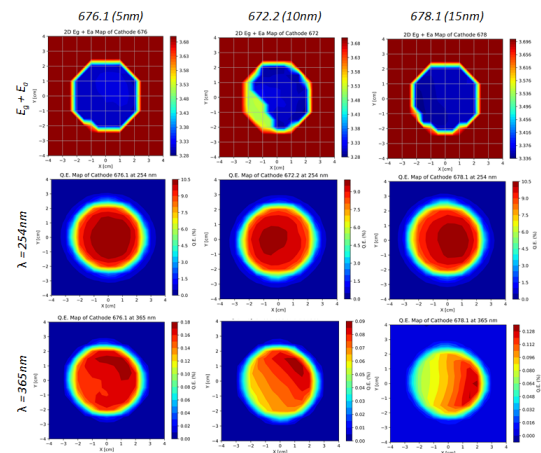


Figure 5: Maps of $E_g + E_a$ (top row), QE at 254 nm (middle row) and 365 nm (bottom row).

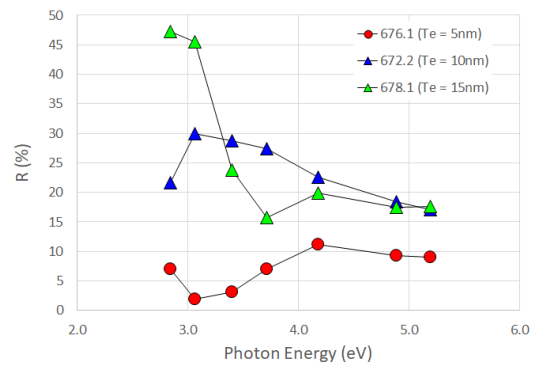


Figure 6: Final reflectivity of the three different films.

Table 3: Photocathode Parameters Summary at 254 nm

	Te [nm]	Cs [nm]	QE [%]	R [%]	$E_g + E_a$ [eV]
676.1	5.1	33.9	12.9	9.3	3.31
672.2	9.8	63.6	11.5	18.4	3.34
678.1	15.1	92.3	12.7	17.5	3.37

CONCLUSION

The photocathodes with different Te thicknesses are quite reproducible and well comparable with films of similar thickness we measured in a previous set. The reflectivity at different wavelengths is a valuable tool for understanding the film growth. To further explore this possibility, we plan to grow even thicker films to have additional information from this optical technique. It will be interesting to learn from measurements at PITZ in the RF Gun environment if any difference will distinguish these three films in terms of lifetime and thermal emittance, having similar properties despite the different Te thicknesses.

REFERENCES

- [1] C. Pagani, P. Michelato, L. Monaco, and D. Sertore, "LASA Cs_2Te Photocathodes: The Electron Source for XFELs", in

Content from this work may be used under the terms of the CC BY 3.0 licence (© 2019). Any distribution of this work must maintain attribution to the author(s), title of the work, publisher, and DOI

Toward a Science Campus in Milan, Ed. Springer, 2018, pp. 281-292.

- [2] S. Lederer, S. Schreiber, L. Monaco, and D. Sertore, "Update on the Photocathode Lifetime at FLASH and European XFEL", presented at the 39th Int. Free Electron Laser Conf. (FEL'19), Hamburg, Germany, Aug. 2019, paper WEP047.
- [3] L. Monaco, P. M. Michelato, C. Pagani, and D. Sertore, "On-Line Diagnostic during Cs2Te Photocathodes Formation", in *Proc. 23rd Particle Accelerator Conf. (PAC'09)*, Vancouver, Canada, May 2009, paper MO6RFP072, pp. 536-538.
- [4] P. W. Huang *et al.*, "Test of Cs2Te Thickness on Cathode Performance at PITZ", presented at the 39th Int. Free Electron Laser Conf. (FEL'19), Hamburg, Germany, Aug. 2019, paper WEP062.
- [5] D. Sertore, A. Bonucci, J. H. Han, P. Michelato, L. Monaco, and S. Schreiber, "Review of the Production Process of TTF and PITZ Photocathodes", in *Proc. 21st Particle Accelerator Conf. (PAC'05)*, Knoxville, TN, USA, May 2005, paper MOPB009, pp. 671-673.
- [6] Edward D. Palik, *Handbook of Optical Constants of Solids*, Academic Press, 1985
- [7] A. diBona *et al.*, "Auger and x-ray photoemission spectroscopy study on Cs2Te photocathodes", *J. Appl. Phys.*, vol. 80, p. 3024, 1996. doi:10.1063/1.363161
- [8] L. Monaco, P. M. Michelato, C. Pagani, and D. Sertore, "Multiwavelengths Optical Diagnostic during Cs2Te Photocathodes Deposition", in *Proc. 1st Int. Particle Accelerator Conf. (IPAC'10)*, Kyoto, Japan, May 2010, paper TUPEC006, pp. 1719-1721.
- [9] D. Sertore, P. Michelato, L. Monaco, and C. Pagani, "A Study for the Characterization of High QE Photocathodes", in *Proc. 22nd Particle Accelerator Conf. (PAC'07)*, Albuquerque, NM, USA, Jun. 2007, paper THPMN024, pp. 2760-2762.
- [10] Evan O. Kane, "Theory of photoelectric Emission from Semiconductors", *Phys. Rev.*, vol. 127, p. 131, 1962. doi:10.1103/PhysRev.127.131